Variability of moisture recycling using a precipitationshed framework

P. W. Keys[1,2], E. A. Barnes[2], R. J. van der Ent[3], and L. J. Gordon[1]

[1]Stockholm Resilience Centre, Stockholm University, Stockholm, Sweden
[2]Department of Atmospheric Science, Colorado State University, Fort Collins, USA
[3]Department of Water Management, Faculty of Civil Engineering and Geosciences, Delft University of Technology, Delft, the Netherlands

*Correspondence to:* P. W. Keys (patrick.keys@su.se)

Abstract. Recent research has revealed that upwind land-use changes can significantly influence downwind precipitation. The precipitationshed (the upwind ocean and land surface that contributes evaporation to a specific location's precipitation) may provide a boundary for coordination and governance of these upwind–downwind water linkages. We aim to quantify the variability of the precipitationshed boundary to determine whether there are persistent and significant sources of evaporation for a given region's precipitation. We identify the precipitationsheds for three regions (i.e., western Sahel, northern China, and La Plata) by tracking atmospheric moisture with a numerical water transport model (Water Accounting Model-2layers, or WAM-2layers) using gridded fields from both the ERA-Interim (European Reanalysis Interim) and MERRA (Modern-Era Retrospective Analysis for Research and Applications) reanalyses. Precipitationshed variability is examined first by diagnosing the persistence of the evaporation contribution and second with an analysis of the spatial variability of the evaporation contribution. The analysis leads to three key conclusions: (1) a core precipitationshed exists; (2) most of the variance in the precipitationshed is explained by a pulsing of more or less evaporation from the core precipitationshed; and (3) the reanalysis data sets agree reasonably well, although the degree of agreement is regionally dependent. Given that much of the growing-season evaporation arises from within a core precipitationshed that is largely persistent in time, we conclude that the precipitationshed can potentially provide a useful boundary for governing land-use change on downwind precipitation.

1 Introduction

Moisture recycling is the phenomenon of evaporation traveling through the atmosphere and returning as precipitation downwind (e.g., Koster et al., 1986; Eltahir and Bras, 1994; Savenije, 1995; Gimeno et al., 2012). Studies of continental moisture recycling, whereby evaporation from land upwind returns as precipitation to land downwind, conclude that a large fraction of the global land surface receives precipitation that was evaporated from other land surfaces (e.g., Lettau et al., 1979; Yoshimura et al., 2004; Dirmeyer et al., 2009; van der Ent et al., 2010; Goessling and Reick, 2013). Some of these studies specifically focus on the possibility that land-use change can impact terrestrial moisture recycling and therefore rainfall in different regions (e.g., Dominguez et al., 2009; Bagley et al., 2012; Tuinenburg et al., 2012; Bagley et al., 2014; Lo and Famiglietti, 2013; Rios-Entenza and Miguez-Macho, 2013; Salih et al., 2013; Wei et al., 2013). In order to understand the spatial patterns of regions that potentially can influence rainfall elsewhere, Keys et al. (2012) introduced the concept of the *precipitationshed*: the upwind ocean and land surface that contributes evaporation to a specific location's precipitation (see Fig. 1). The precipitationshed concept has previously been used to highlight several regions in the world where local livelihoods are closely dependent on rainfed ecosystems, and why land-use changes in these regions' precipitationsheds could have significant consequences for these societies.
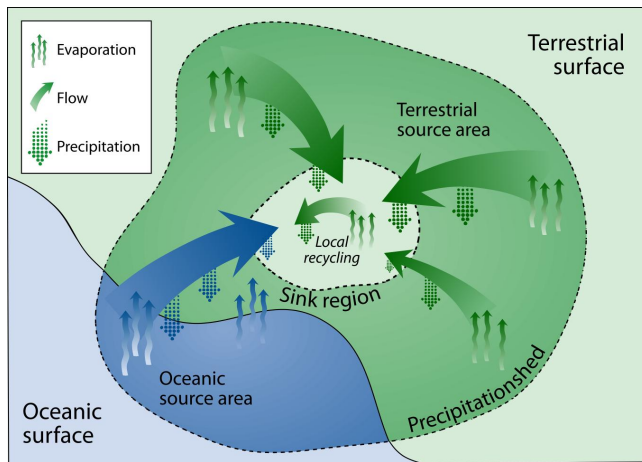
Figure 1. Conceptual precipitationshed; reprinted from Keys et al. (2012), published in Biogeosciences in 2012 (shared under the Creative Commons Attribution 3.0 License).

Moisture recycling has been explored by previous studies on both seasonal and interannual timescales, and at both global and regional spatial scales. At large spatial scales, mid- and high-latitude continental regions tend to experience continental (i.e., terrestrial) moisture recycling, while low-latitude regions are more strongly influenced by oceanic sources of moisture (e.g., Koster et al., 1986; Numaguti, 1999). Other work has suggested that proximity to coastal regions increases the fraction of moisture of oceanic origin (e.g., Risi et al., 2013). At both global and regional spatial scales, moisture recycling in wet years and dry years can be substantially different (e.g., Dirmeyer et al., 2013b). For example, sub-Saharan wet season precipitation may be more directly related to divergence and convergence of moisture over continental regions upwind, rather than evaporation rates in adjacent regions of the Atlantic Ocean (e.g., Druyan and Koster, 1989). Likewise, in the Mississippi River basin, oceanic evaporation dominates wet-year precipitation, while local, continental evaporation is important during dry years (e.g., Brubaker et al., 2001; Chan and Misra, 2010). In the Amazon, many studies suggest that, though advection of oceanic moisture is a very important source of precipitation, terrestrial recycling is also a very important process for sustaining regional rainfall (e.g., Eltahir and Bras, 1994; Bosilovich and Chern, 2006; Drumond et al., 2008; Gimeno et al., 2012; Spracklen et al., 2012). Large-scale modes of climate variability, such as the North Atlantic Oscillation or the El Niño–Southern Oscillation (ENSO) have also been shown to have marked effects on moisture recycling variability (e.g., Sodemann et al., 2008; van der Ent and Savenije, 2013).

Global moisture recycling analyses commonly use global climate reanalysis data, with each data set having different strengths and weaknesses. Previous studies have focused on the differences in precipitation and evaporation between reanalysis data, illustrating some discrepancies (e.g.,

Bosilovich et al., 2011; Rienecker et al., 2011; Lorenz and Kunstmann, 2012). Trenberth et al. (2011) provide a comprehensive comparison of global atmospheric moisture transport from ocean to land across multiple reanalysis data sets, focusing primarily on the ERA-Interim (European Reanalysis Interim) and MERRA (Modern-Era Retrospective Analysis for Research and Applications) reanalyses. However, less is known about the sensitivity of specific upwind–downwind moisture recycling dynamics (i.e., the precipitationshed) to specific reanalysis data.

In order to determine whether the precipitationshed is a useful tool for relating upwind land use with downwind precipitation, the underlying variability of moisture recycling must be quantified. In this work we capture moisture recycling relationships using a precipitationshed framework to quantify variability in time and space. Specifically, we aim to address three main questions:

1. How do precipitationsheds differ between reanalysis data sets?

2. Are there core areas of a given sink region's precipitationshed that persistently contribute significant volumes of evaporation every year?

3. How do precipitationsheds vary on interannual timescales?

We first analyze how different data sets influence the mean precipitationshed by comparing two different reanalysis data products. We then explore the dominant spatial patterns of precipitationshed variability through time (i.e., 1979 to 2012). This is done for three specific precipitation sink regions, using two different methods. The first method is a diagnostic that identifies the frequency of significant evaporation contribution from throughout the precipitationshed. The second method is a statistical analysis which identifies the spatial patterns of variance of evaporation contribution. Our results will be presented for three specific regions, but the techniques used in this analysis can be applied to any region of the globe.

2   Methods

2.1   Sink regions

We analyze precipitationshed variability for three different regions: (a) western Sahel (including Burkina Faso and parts of Mali, Niger, Ghana, and Mauritania), (b) northern China, and (c) La Plata (named for the La Plata river basin, including parts of Brazil, Argentina, Paraguay, and Uruguay); these regions are depicted in Fig. 2 and are considered *terrestrial moisture recycling dependent* under the criteria that

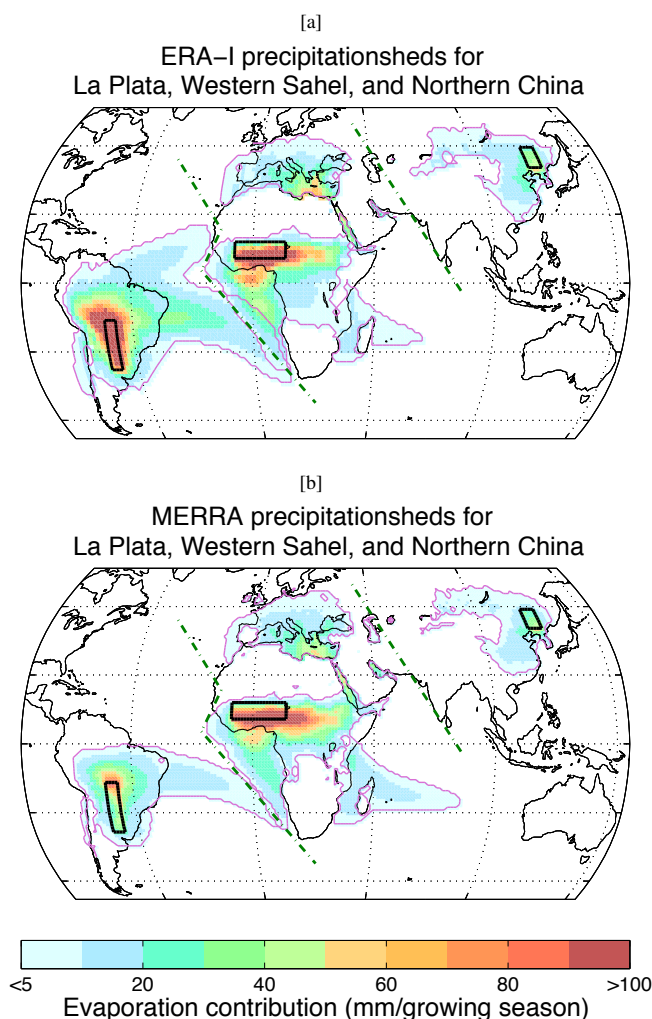– terrestrial evaporation sources provide >50 % of growing-season precipitation

– rainfed agriculture is important for a large fraction of the population.

These sink regions are a slightly modified subset of those found in Keys et al. (2012), with key characteristics listed in Table 1. The sink regions vary in terms of their location on the planet, climate zone, growing-season months, and growing-season precipitation. This range of characteristics allows us to understand how precipitationshed variability manifests in different parts of the world, during different times of the year, and under different large-scale meteorological conditions.

2.2 Data

We use climate data from the ERA-Interim (ERA-I) reanalysis (Dee et al., 2011), and from the MERRA (Bosilovich et al., 2011). Recent evaluations of ERA-I and MERRA have shown that both ERA-I and MERRA reproduce precipitation reasonably well over land (e.g., Trenberth et al., 2011); however, they both have relative strengths and weaknesses in different parts of the world. For example, MERRA underestimates precipitation rates in the central Amazon and within the La Plata river basin (e.g., Dirmeyer et al., 2013b), while ERA-I overestimates precipitation rates along the western side of the Andes, across Congolese Africa, and across the Tibetan Plateau (e.g., Lorenz and Kunstmann, 2012). Despite these issues, ERA-I and MERRA remain among the best available reanalysis products at the time of our analysis (e.g., Rienecker et al., 2011; Trenberth et al., 2011).

For both reanalysis data sets, we analyze 6-hourly model level zonal winds, meridional winds, and relative humidity; 6-hourly surface pressure; and 3-hourly precipitation and evaporation. The data span the time period January 1979 through January 2013 and were downloaded at $1.5° \times 1.5°$ for ERA-I and $1.0° \times 1.25°$ for MERRA. Despite higher-spatial-resolution data being available, the ERA-I $1.5° \times 1.5°$ data were used for computational efficiency, and the MERRA $1.0° \times 1.25°$ data were used because the variables required for the Water Accounting Model-2layers (WAM-2layers) were only available at $1.0° \times 1.25°$ resolution. During the analysis process, we discretize the data to a 15 min time step to limit numerical errors in the backtracking calculation. We complete the discretization using a linear interpolation from the 6- and 3-hourly data to 15 min intervals. It is possible that our linear interpolation hides temporal heterogeneity, particularly in the evaporation and precipitation fields. However, since we perform our analysis on the aggregated monthly data, rather than daily or sub-daily data, we are confident that any potential small-scale temporal heterogeneities are overwhelmed by larger-scale phenomena at the monthly timescale and beyond. We use the January 2012–January 2013 data as spin-up for the backtracking calculation but exclude it from the analysis. Additionally, given that one potential application of these methods is to understand the variability of moisture recycling regimes relevant to rain-

[a]
ERA–I precipitationsheds for
La Plata, Western Sahel, and Northern China

[b]
MERRA precipitationsheds for
La Plata, Western Sahel, and Northern China

<5   20   40   60   80   >100
Evaporation contribution (mm/growing season)

Figure 2. Comparison of mean precipitationshed extents for ERA-Interim (top) and MERRA (bottom), for the period 1980–2011. Lines are included to identify the sink region (black box) the $5\,mm\,growing\,season^{-1}$ precipitationshed boundary (magenta line), and to separate the different precipitationsheds, since the three precipitationsheds do not occur simultaneously (dashed green line). Note that, where the $5\,mm\,growing\,season^{-1}$ boundaries for the western Sahel and La Plata basin overlap (particularly in the South Atlantic), the values for the western Sahel are displayed, and the Mediterranean sources belong to the western Sahel. Values less than 5 mm are excluded from the precipitationsheds.

fed ecosystem services in these sink regions, we limit the scope of the analysis to the sink-specific, growing-season months as shown in Table 1. These growing-season months were identified following Portmann et al. (2010) and Keys et al. (2012). Also, given that growing seasons in the South Hemisphere occur across two calendar years, we assign the year of the growing season using its final month. For example, the 2011 growing season for the La Plata sink region would span November and December of 2010 as well as January, February, and March of 2011. As a result of this, we

Table 1. Characteristics of sink regions (P is precipitation, and gs is growing season). "Total P" refers to the 32-year mean precipitation (in mm) during the growing season.

Sink region	Köppen–Geiger climate zone	Growing season	Total P [mm gs^{-1}]	Total P from land [mm gs^{-1} (%)]
Western Sahel	Arid, steppe	Jun–Oct	549	307 (56 %)
Northern China	Snow, winter dry	May–Sep	464	320 (69 %)
La Plata basin	Warm, fully humid	Nov–Apr	826	512 (62 %)

exclude the year 1979 for the Northern Hemisphere sink regions to ensure that they have the same number of growing seasons as the Southern Hemisphere sink region. Thus, we have 32 years to define a climatology and perform the analysis for each data set.

2.3 WAM-2layers

In order to study the variability of precipitationsheds, we backtrack moisture when it enters the atmosphere as evaporation and ending where the moisture falls out of the atmosphere as precipitation. We use the WAM-2layers (version 2.3.01), which tracks atmospheric moisture both forward and backward in time. The WAM-2layers tracks the volume of evaporation and precipitation that enters and exits (respectively) a column of air above a parcel of land. As the model integrates forward in time, the moisture in each column moves horizontally and vertically between grid cells, advected by the prevailing winds. At each time step WAM-2layers computes the water balance of both total and "tagged" moisture in each grid cell, in a lower and upper atmospheric bucket. Thus, this is an Eulerian method for tracking moisture. In this paper we are tracking tagged precipitation from a location of interest back in time. Precipitation enters and evaporation exits our atmospheric water buckets. Moisture is moved horizontally and vertically between grid cells by multiplying them with wind speeds. In this way, by the end of a model run, there is a long output record of moisture fluxes that have flowed between the land surface and the atmosphere. The model has been updated since its original 2-D configuration (van der Ent et al., 2010), to a 3-D configuration that tracks two layers of atmospheric water vapor. The primary advantage of using the two-layer version is that we capture the variation in the speed of moisture transport in the upper and lower atmosphere by better resolving wind shear (van der Ent et al., 2013). For a detailed description of the WAM-2layers, refer to van der Ent et al. (2013, 2014).

2.4 Precipitationshed boundary definition

The precipitationshed analysis requires identifying a boundary based on evaporation contribution. Previous work defined the precipitationshed boundary using the fraction of total evaporation contribution to a given sink region, e.g.,

70 % of source evaporation for a given sink region's precipitation (Keys et al., 2012). This previous work also examined the difference between *absolute* (e.g., 5 mm) and *relative* (e.g., 50 % of evaporation from a grid cell) evaporation contribution. For this analysis, we use a *significant contribution* definition, whereby an absolute evaporation contribution of 5 mm or more per growing season from a given grid cell constitutes a meaningful depth of precipitation in the sink region. We explored the sensitivity of the precipitationshed boundary to small variations in the significant contribution parameter, and we found that our results were insensitive to these variations. It is important to note that the previously used method of "fraction of total evaporation contribution" (Keys et al., 2012) and the "significant contribution" method we use herein are both user-defined and that the significance values may be chosen differently based on the question being asked.

2.5 Statistical methods

2.5.1 Mean precipitationshed difference

In our analysis we compare the mean precipitationsheds for each sink region, between the two driving reanalyses ERA-I and MERRA, first using a merged map of the precipitationsheds and then by calculating the evaporation contribution difference between the two data sets. This difference helps determine whether ERA-I or MERRA contributes more evaporation. We calculate this difference, D, in evaporation contribution, E_C, as

$$D = \frac{E_{C,ERA} - E_{C,MERRA}}{E_{C,ERA}}, \tag{1}$$

where $E_{C,ERA}$ is ERA-I evaporation contribution, $E_{C,MERRA}$ is MERRA evaporation contribution, and we divide their difference by $E_{C,ERA}$. The decision to compute the difference with respect to ERA-I is arbitrary.

2.5.2 Precipitationshed variability

We quantify precipitationshed variability using two metrics: (1) a measure of persistence and (2) a measure of variance. First, the persistence measure identifies which regions of the precipitationshed persistently contribute significant amounts

of evaporation to the sink region. The *persistence* of a given grid cell is the fraction of years the evaporation contribution exceeds the significant threshold of 5 mm growing season^{-1}. Thus, the persistence, P_i, of a precipitationshed is the number of years, N, for which

$$E_{C,i,t} > S, \tag{2}$$

where E_C is the evaporation contribution; i, t is the spatial and temporal indices for all grid cells; and S is the significant contribution threshold, here 5 mm growing season^{-1}. Additionally, since we are trying to identify the most persistent sources of evaporation, we define the *core precipitationshed* as the evaporation source region that contributes above the significant threshold for all 32 years.

The second measure of precipitationshed variability uses empirical orthogonal function (EOF) analysis to quantify the growing-season average evaporation variability over the precipitationshed. EOF analysis has a long history of use in the atmospheric science community and is often used to define climate indices associated with large-scale atmospheric variability (e.g., Hartmann and Lo, 1998; Thompson and Wallace, 1998). EOF analysis outputs a spatial pattern (the EOF) that represents the anomalies that explain the most variance of the field of interest. The first EOF always accounts for the most variance, with each subsequent EOF accounting for less and less of the total variance of the field. In this work, we use EOF analysis to quantify the anomalous evaporation patterns that explain the most variance in the evaporation contribution to a given sink region. In other words, each EOF provides the pattern of anomalous evaporation that best explains differences in the evaporation contribution across different years.

Before performing the EOF analysis, we remove the long-term linear trend in evaporation contribution at each grid point. This is done by taking the total precipitationshed evaporation contribution for each growing season, calculating its linear least-squares fit, and removing it from the data. We remove this long-term trend to ensure that the variability we are capturing is representative of interannual variability and not simply due to long-term trends. We then perform the EOF analysis for each sink region's de-trended, total growing-season evaporation contribution. The determination of whether a specific EOF is significantly different from adjacent EOFs is determined using methods described in North et al. (1982), and we limit our focus to the first two EOFs for each region.

3 Results

Results are presented in the following section, beginning with the comparison of mean precipitationsheds between reanalysis data sets, followed by a discussion of precipitationshed persistence, and finishing with the results of the EOF analysis.

### 3.1 Comparison of the mean precipitationshed between reanalyses

First, we compare the mean precipitationsheds for the three sink regions (depicted as black boxes in Fig. 2), for both ERA-I and MERRA. Recall that a precipitationshed depicts the grid cells that contribute evaporation to a given sink region's precipitation, during a specific period of time.

The most important evaporation source regions in the ERA-I western Sahel precipitationshed come from the Gulf of Guinea, the entire east–west expanse of the Sahel, and the Mediterranean Sea (Fig. 2a). Also, central Africa, including parts of the Congo River basin, coastal Mediterranean regions (e.g., Greece, southern Italy, and western Turkey), and the Mozambique Channel (between Mozambique and Madagascar) are important sources of evaporation. The results for MERRA indicate generally good agreement with ERA-I, despite a few notable differences. Somewhat less contribution appears to come from the Gulf of Guinea, while significantly more comes from east Africa (including Sudan, Ethiopia, and Kenya), as well as from the Indian Ocean around the northern half of Madagascar and adjacent to Tanzania.

In the western Sahel difference calculation (Sect. 2.5.1, Fig. 3a), ERA-I has between 10 and 40 % higher contributions compared to MERRA from the Gulf of Guinea, the Mediterranean, the central Sahel, and the Congo River basin. Conversely, MERRA has up to 100 % higher evaporation contributions for central Africa, including Cameroon, Central African Republic, South Sudan, and Ethiopia.

For northern China, the ERA-I precipitationshed indicates significant local sources of evaporation throughout northwest China, and as far south as Shanghai and west to Xi'an. Additional evaporation contribution appears to come from the Mongolian Steppe and the Korean Peninsula. The general precipitationshed pattern for MERRA is very similar, with somewhat less evaporation contribution coming from the Mongolian Steppe and China's central coast. For the northern China difference calculation (Fig. 3b), source regions in the ERA-I data set are generally 0–30 % larger than MERRA, while scattered regions in western Mongolia, central China, and the Korean Peninsula are 0–40 % larger in MERRA.

For the La Plata sink region, important evaporation sources in ERA-I include the southern Amazon basin and the entire La Plata river basin (including Uruguay, Paraguay, Bolivia, and northern Argentina). Additionally, the central and South Atlantic Ocean is an important source of evaporation. There is also a small source region on the west side of the Andes, adjacent to northern Chile. The results for MERRA indicate an order-of-magnitude reduction in evaporation contribution from nearly all evaporation source regions, with some large differences in the overall precipitationshed spatial pattern. A distinctive feature of the MERRA precipitationshed is much lower North Atlantic evaporation contribution, consistent with the lower-than-observed precipitation difference discussed by Lorenz and Kunstmann (2012).

[a]
West Sahel

[b]
North China

[c]
La Plata

Percent difference between ERA–I and MERRA
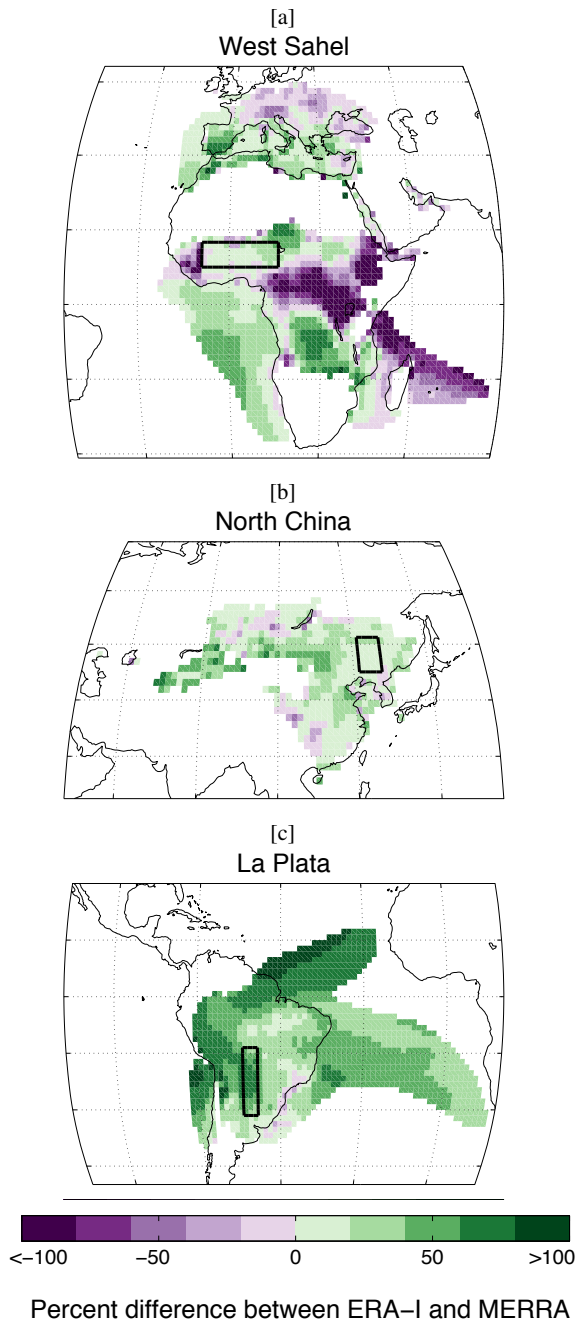
Figure 3. Difference between ERA-I and MERRA precipitationsheds (see Fig. 2), as a fraction of the ERA-I value (see calculation in Sect. 2.5.1), for the years 1980–2011. Green colors indicate where ERA-I source evaporation is larger, and purple colors indicate where MERRA source evaporation is larger.

The difference calculation reveals the high level of disagreement between ERA-I and MERRA in the La Plata sink region's precipitationshed (Fig. 3c). The difference indicates from 20 to > 100 % more evaporation is coming from ERA-I relative to MERRA, but it is worth repeating that the MERRA evaporation contribution in this region is very low;

so even though ERA-I is nearly double the MERRA value in some of these places, it is likely due to the very low absolute contributions from MERRA.

To summarize, there is a high level of agreement between ERA-I and MERRA in capturing the mean precipitationsheds for the western Sahel and northern China. For the La Plata precipitationshed we see both a systematic underestimation of evaporation contribution in MERRA relative to ERA-I and a significantly different spatial pattern between the two precipitationsheds.

3.2 Precipitationshed persistence

Next, we explore the precipitationshed persistence results focusing primarily on the ERA-I results, with additional figures for MERRA in Fig. S1 in the Supplement. Recall that the persistence of a given grid cell is the fraction of years the evaporation contribution exceeds the significant threshold of $5\,\mathrm{mm}\,\mathrm{growing\,season}^{-1}$. We first examine the core precipitationshed, where grid cell persistence is 100 %, and then explore lower levels of persistence.

The western Sahel core precipitationshed (Fig. 4a) covers much of the Sahel, central Africa, the Congo River basin, the Gulf of Guinea, southern and eastern Europe, the Mediterranean and Red seas, and the Persian Gulf. More than three-quarters of mean growing-season precipitation (82 %) comes from the core precipitationshed, with half (50.1 %) coming from terrestrial core regions (see Table 2, columns 5 and 6). As the persistence falls below 100 % of years, new source regions emerge in the Great Lakes region of Africa, and the Indian Ocean east of Madagascar. The MERRA results are largely consistent with the ERA-I results (Table 2 and Fig. S1a in the Supplement).

The northern China core precipitationshed (Fig. 4b) occupies a region to the southwest of the sink region, including densely populated urban areas (e.g., Beijing, Shanghai), the North China Plains, and the eastern Mongolian Steppe. The core precipitationshed also includes the entire Korean Peninsula and much of the Chinese and Russian portions of the Amur River basin. As the persistence decreases, the source regions expand north and south, but this expansion is small relative to the spatial extent of the core precipitationshed. Just under half of mean growing-season precipitation (45.5 %) originates from the core precipitationshed, with nearly all (43.9 %) originating from terrestrial core areas. This implies that over half (54.5 %) of precipitation originates from upwind areas contributing less than $5\,\mathrm{mm}\,\mathrm{growing\,season}^{-1}$. As with the western Sahel comparison, the MERRA results largely agree with the ERA-I results (Table 2 and Fig. S1b in the Supplement).

The core precipitationshed for the La Plata sink region (Fig. 4c) covers much of the South American continent, including nearly the entire Amazon and La Plata river basins, north to the Guiana Shield, as far south as the edge of Patagonia, and a narrow band of oceanic contribution from the

Table 2. Depths of precipitation (in mm growing season^{-1}) provided by the corresponding precipitationshed; fractions of total are indicated in parentheses. Note that "precipitation" is abbreviated to P, and "precipitationshed" is abbreviated to "Pshed".

Sink region	Total P	5 mm Pshed	Sink region	Core Pshed	Core Pshed (Land only)
ERA-I					
Western Sahel	549	458 (83.3 %)	102 (18.7 %)	451 (82.0 %)	275 (50.1 %)
Northern China	464	213 (45.9 %)	3 (8 %)	211 (45.5 %)	204 (43.9 %)
La Plata basin	826	717 (86.8 %)	140 (16.9 %)	713 (86.4 %)	496 (60 %)
MERRA					
Western Sahel	579	474 (81.7 %)	92 (16.0 %)	463 (79.8 %)	309 (53.3 %)
Northern China	442	191 (43.3 %)	3 (7.8 %)	185 (41.8 %)	180 (40.7 %)
La Plata basin	337	252 (74.6 %)	43 (13.4 %)	240 (71.2 %)	190 (56.2 %)

west side of the Chilean Andes. There is also a small lobe of contribution from the equatorial Atlantic Ocean, and a large lobe of evaporation contribution from the South Atlantic Ocean, extending nearly to the Cape of Good Hope in South Africa. More than three-quarters of growing-season precipitation (86.4 %) comes from the core precipitationshed, while over half (60 %) comes from the terrestrial portions. Unlike the western Sahel and northern China persistence analysis, there are notable differences in the La Plata persistence identified by ERA-I and MERRA. The reasons have already been discussed in Sect. 3.1, but it is worth repeating that the core precipitationshed shape (i.e., spatial pattern), area, and volume of contribution are all much smaller for MERRA than ERA-I (Table 2 and Fig. S1c in the Supplement).

A composite of the core precipitationsheds for the three sink regions, and both reanalyses, is depicted in Fig. 5. It is clear that for the western Sahel core precipitationshed there is a high level of agreement between ERA-I and MERRA (i.e., the red areas in Fig. 5). There are a few differences, such as ERA-I including more of equatorial Africa, the Mozambique Channel, and the Iberian Peninsula. Likewise, the MERRA result includes additional regions in Ethiopia and central Europe. For the northern China composite, we see generally good agreement, with ERA-I including more contributions from the Mongolian Steppe, while MERRA's unique features are negligible.
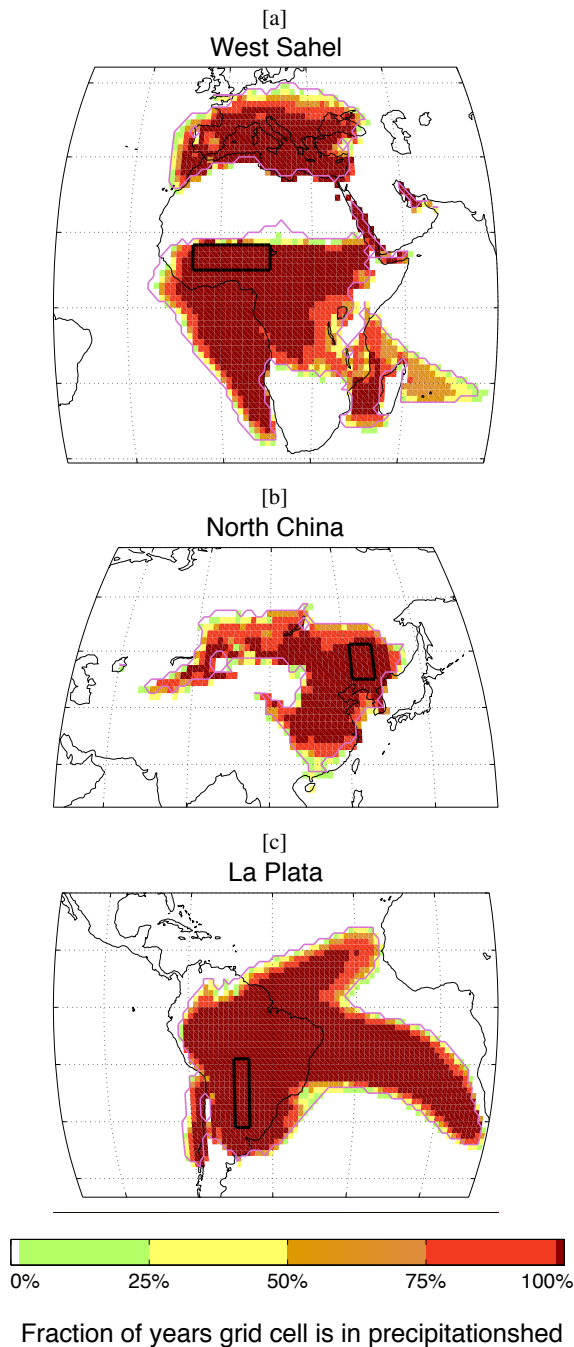
There is a clear contrast between the La Plata sink region's ERA-I and MERRA core precipitationsheds. MERRA's overlap with ERA-I falls entirely within the ERA-I core precipitationshed. A key aspect of this pronounced disagreement

is the fact that both the northern Amazonian and Atlantic Ocean contributions present in ERA-I are almost entirely absent in MERRA. This finding is consistent with previous results above that suggest a systematic underestimation of evaporation magnitudes in MERRA throughout the La Plata region.

In summary, prior to this analysis it was uncertain whether or not precipitationsheds tended to be highly variable, such that every year the rain came from different evaporation sources. However, our results clearly show that this is not the case and that the core precipitationshed both is largely persistent over a very large spatial domain and, in general, captures around 50 % or more of growing-season precipitation falling in the sink regions.

3.3   EOF analysis

Next, we employ EOF analysis to reveal the spatial patterns that explain the most variance in the three precipitationsheds. As stated earlier in Sect. 2.5.2, the variable we are analyzing is growing-season average evaporation. EOF1 for the western Sahel (Fig. 6) shows an EOF spatial pattern with only positive anomalies, implying that anomalous evaporation contribution to the sink region is best explained by an increase or decrease in evaporation contribution in the regions with warmer colors. The sign of the anomalies in the EOF are arbitrary and, thus, should not be interpreted as "positive" or "negative" but rather as corresponding to alternating phases present in the data. Thus, this *pulsing* in the evaporation contribution depicted by EOF1 is dominated by

[a]
West Sahel

[b]
North China

[c]
La Plata

0%   25%   50%   75%   100%

Fraction of years grid cell is in precipitationshed

Figure 4. The persistence of the western Sahel, northern China, and La Plata precipitationsheds for ERA-I, for the years 1980–2011. "Significant" is defined as greater than 5 mm growing season^{-1}, and the dark red areas correspond to the *core precipitationshed*, with significant contribution occurring during 100 % of growing seasons. The black boxed areas are the sink regions for each precipitationshed.

evaporation from the Sahel (centered over Niger) and from the Gulf of Guinea. Much less variance appears to be explained by the rest of continental Africa. Thus, variations in

Composite of core precipitationsheds for
La Plata, Western Sahel and Northern China

ERA–I only   MERRA only   ERA–I & MERRA
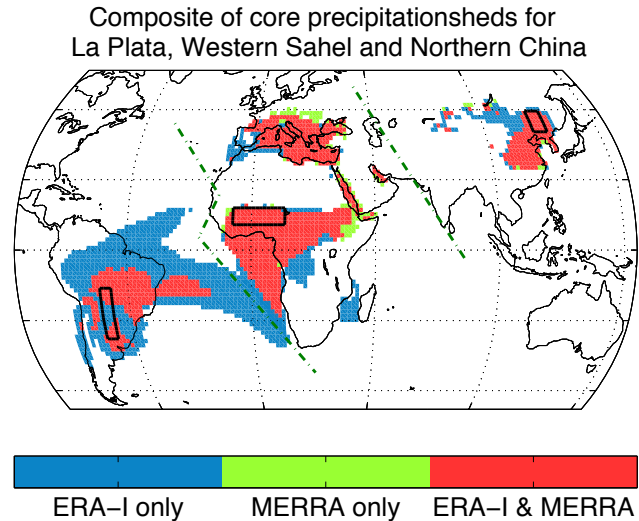
Figure 5. Comparison of core precipitationshed extents for ERA-Interim and MERRA results, for the period 1980–2011, using the > 5 mm growing season^{-1} boundary and 100 % occurrence. The dashed green lines are meant to visually separate the different precipitationsheds. Note that, where the core precipitationshed boundaries for the western Sahel and La Plata basin overlap (particularly in the South Atlantic), the values for the western Sahel are displayed. Also, the Mediterranean sources belong to the western Sahel precipitationshed.

terrestrial evaporation over the Sahel account for the most variance in the precipitation contribution over the western Sahel.

EOF2 for the western Sahel accounts for considerably less variance (Fig. 6), with the EOF anomaly pattern indicating a shifting of the evaporation contribution from west Africa and the Gulf of Guinea to central Africa or, equally, from central Africa to west Africa and the Gulf of Guinea. Thus, a shifting of evaporation contribution between these two regions accounts for the second-most variance of the precipitationshed contribution to the western Sahel from one growing season to the next. Also, we note that this shifting pattern resembles a response to oscillations in larger-scale climate phenomena, like ENSO or Mediterranean sea surface temperature (SST) anomalies, and thus these climate phenomena could play a role in driving the precipitationshed variability depicted in EOF2 (e.g., Rowell, 2003; van der Ent et al., 2012; Giannini et al., 2013).

The MERRA-generated EOF1 (Fig. 6) for the western Sahel shows a slightly different pattern from that of ERA-I, with the anomalous evaporation contribution extending over a large region across the Sahel and central Africa, as well as the Gulf of Guinea. In particular, MERRA's EOF1 has much more anomalous evaporation contribution originating from Sudan, South Sudan, Chad, Niger, Central African Republic, and from the sink region itself in the western Sahel. There remains an important source in the Gulf of Guinea, but this
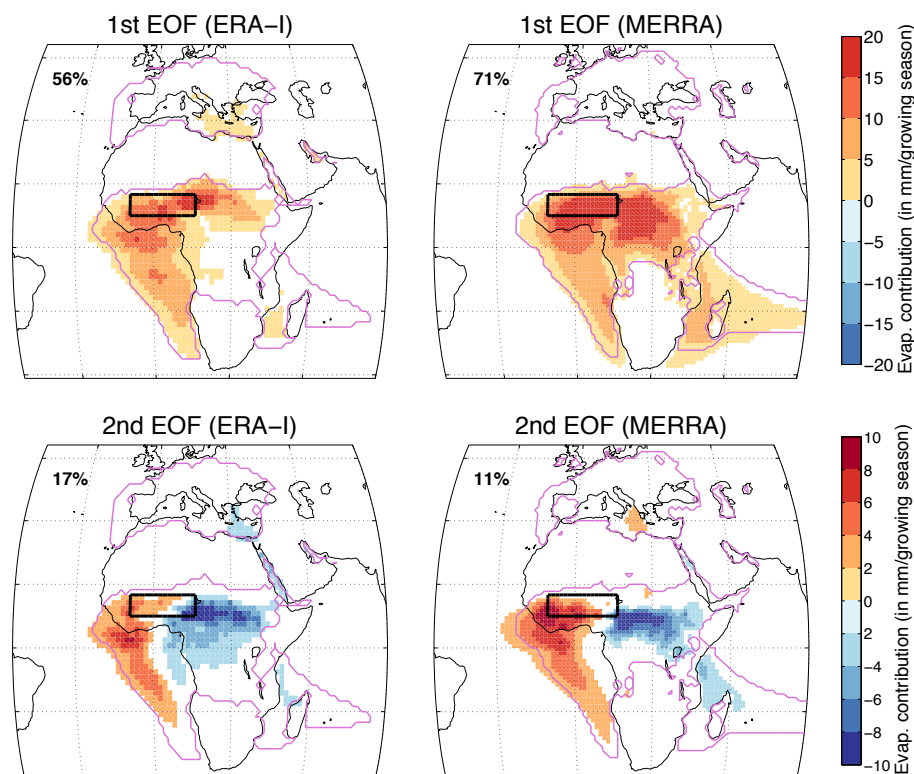
Figure 6. Comparison of first and second EOFs for the western Sahel (ERA-Interim on left and MERRA on right), for the period 1980–2011. The magenta line indicates the $5\,\text{mm}\,\text{growing season}^{-1}$ precipitationshed boundary, the black box indicates the sink region, and the bold number in the upper left corner indicates the amount of variance explained by the associated pattern. We do not show values $< 2\,\text{mm}\,\text{growing season}^{-1}$, for the sake of clarity in the figure.

is complemented by an additional anomalous source in the Mozambique Channel between Mozambique and Madagascar. MERRA's EOF2 (Fig. 6) resembles ERA-I's EOF2, with a similar pattern of shifting anomalies. However, MERRA's anomaly over central Africa is considerably more concentrated over Central African Republic, South Sudan, and Ethiopia, with almost no anomalous contribution originating in the Congo River basin.

The northern China EOFs are plotted in Fig. 7. EOF1 accounts for just over half of the growing-season variance for ERA-I (Fig. 7), and the pattern suggests a pulsing of evaporation from Manchuria and eastern China with a small lobe of anomalous contribution extending west across the Mongolian Steppe. Also, the highest evaporation contribution anomalies occur within the sink region itself. Very little anomalous evaporation comes from the desert regions of western China, likely due to the very low evaporation rates there. Despite some regions of China being more influenced by the East Asian Monsoon or Tibetan Plateau evaporation dynamics (e.g., Ding and Chan, 2005), EOF1 suggests that the anomalous evaporation contribution is most strongly explained by local, rather than more distant, evaporation variability. EOF2 for northern China (Fig. 7) accounts for much less variance (13 %) and indicates a very weak

shifting pattern between (a) northern China and (b) the mouth of the Yangtze River, though the Yangtze anomaly is not depicted in our figure because the values are so small (less than $2\,\text{mm}\,\text{growing season}^{-1}$).

MERRA's EOF1 is quite similar to ERA-I (Fig. 7), with 58 % of the variance explained and with a very similar spatial pattern. The only difference is that slightly more of the anomalous evaporation contribution appears to come from the sink region itself in MERRA's EOF1. For EOF2, MERRA's spatial pattern is similar to ERA-I's, though with even less variance explained (Fig. 7). Recall that by definition EOF1 and EOF2 are orthogonal to (i.e., independent of) one another. Thus, even though the spatial patterns in EOF1 and EOF2 (for both ERA-I and MERRA) overlap, the patterns explain separate anomalous evaporation patterns that are uncorrelated.

The La Plata EOFs are plotted in Fig. 8. Before discussing the EOFs for La Plata, it is important to note that the first and second EOFs for the ERA-I precipitationshed are not significantly different, meaning the patterns are likely not robust. Thus, one should exercise considerable caution when interpreting these results. We will therefore only describe the EOFs for the MERRA data set, with the large caveat that ERA-I does not reproduce MERRA's results.
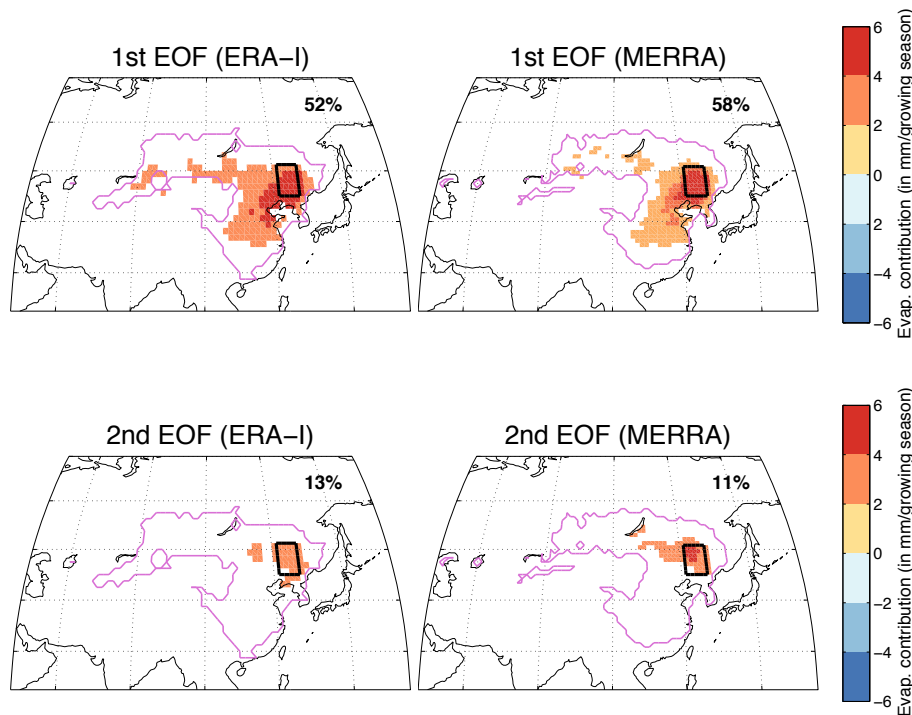
Figure 7. Comparison of first and second EOFs for northern China (ERA-Interim on left and MERRA on right), for the period 1980–2011. The magenta line indicates the $5\,\text{mm}\,\text{growing season}^{-1}$ precipitationshed boundary, the black box indicates the sink region, and the bold number in the upper right corner indicates the amount of variance explained by the associated pattern. We do not show values $<2\,\text{mm}\,\text{growing season}^{-1}$, for the sake of clarity in the figure.

The MERRA EOF1 (Fig. 8) accounts for more than three-quarters of the evaporation variance and shows a pulsing over the southern Amazon and Brazilian savanna, with the largest anomalies coming from regions that happen to be experiencing rapid and large-scale land-use change (e.g., Ferreira-Pires and Costa, 2013). There is also a band of anomalies extending out across the South Atlantic Ocean, suggesting that the terrestrial variations in precipitation in the La Plata sink region are linked to anomalous evaporation contributions from the adjacent Atlantic Ocean. This likely suggests that the dynamical drivers of the Atlantic Ocean anomalies may also drive the terrestrial variability.

EOF2 accounts for a very small fraction of the variance (about 5 %) and indicates a shifting pattern of anomalous evaporation contribution from southern Amazonia to central Brazil. This anomaly appears to follow the gradient between tropical, wet rainforests to the north and drier savannas to the south. The current land-use change dynamics associated with these two regions, namely the expansion of agriculture and the removal of forests, could have implications for the future of this evaporation variability and its contribution to the La Plata region. Nonetheless, given that the pulsing pattern in EOF1 explains an order-of-magnitude more variance than EOF2, the gradient between rainforest and savanna appears to be of much lower relative importance.

To summarize, the leading mode of variability for the three sink regions indicates an anomalous pulsing of evaporation contribution primarily from upwind, terrestrial source regions, whereby either more or less total evaporation enters the sink region from the precipitationshed. This finding should serve to underline the importance of terrestrial sources of moisture for these three sink regions. Additionally, the second mode of variability for all three sink regions generally indicates an anomalous *shifting* of evaporation contribution. Though this pattern accounts for much less of the variance in evaporation contribution across the 32-year period, it may be useful to explore whether these patterns become more important during extreme dry or wet years, since climate-scale oscillations (e.g., ENSO) are often associated with hydrologic extremes.

4 Discussion

4.1 The ERA-I and MERRA precipitationsheds

The over-arching result from our comparison of the reanalyses is that, in general, there is a high correspondence in the spatial patterns of the precipitationsheds, with the caveat that ERA-I tends to have higher evaporation contributions than MERRA. Importantly, the precipitationshed patterns that we

Hydrol. Earth Syst. Sci., 18, 3937–3950, 2014

www.hydrol-earth-syst-sci.net/18/3937/2014/
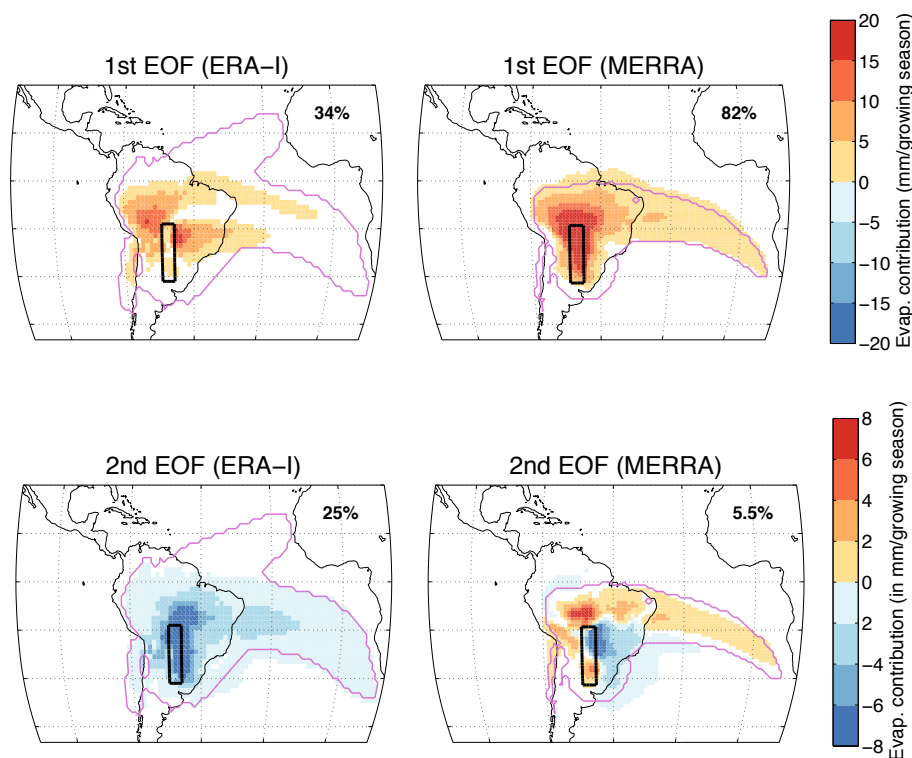
Figure 8. Comparison of first and second EOFs for La Plata (ERA-Interim on left and MERRA on right), for the period 1980–2011. The magenta line indicates the 5 mm growing season^{-1} precipitationshed boundary, the black box indicates the sink region, and the bold number in the upper right corner indicates the amount of variance explained by the associated pattern. We do not show values < 2 mm growing season^{-1}, for the sake of clarity in the figure.

identify broadly echo the findings reported in previous studies, with some slight differences. In the western Sahel precipitationshed we find that ERA-I contributes more moisture than MERRA in the northern Congo, which is consistent with Lorenz and Kunstmann (2012), who assert that ERA-I overestimates precipitation in Congolese Africa. Other studies strongly support the importance of evaporation sources in the Gulf of Guinea and the Mediterranean region (e.g., Reale et al., 2001; Biasutti et al., 2008), which our study also confirms. For northern China, the ERA-I precipitationshed also has higher evaporation contributions than MERRA. This is consistent with findings suggested by Trenberth et al. (2011), who found that during summer months (e.g., July) total column atmospheric water over northern China was higher in ERA-I than in MERRA. The northern China sink region used in Bagley et al. (2012) is shifted south relative to the sink region used in this study, so the spatial pattern of source regions is also shifted south. Nonetheless, our spatial patterns are qualitatively similar, and in both Bagley et al. (2012) and our own work eastern China emerges as an important source region of evaporation.

Finally, for the La Plata precipitationshed, we find both that ERA-I has more moisture in absolute terms and that the important moisture source regions are in the northern Amazon, central Atlantic, and La Plata river basin as compared to the southern Amazon, eastern savanna and lower La Plata river basin in MERRA. This divergent finding is consistent with both Dirmeyer et al. (2013a) and Lorenz and Kunstmann (2012), who found MERRA underestimated precipitation rates in these regions. Interestingly, the South American sink region used in Bagley et al. (2012) also found that the northern Amazon and central Atlantic contributed very little growing-season evaporation. Their work employed the National Centers for Environmental Protection (NCEP) II Renanalysis, which appears to be more similar to MERRA than ERA-I. Given these conflicting findings related to Amazonian moisture transport, future work should exercise caution when drawing conclusions from a single reanalysis data set, and perhaps complement such work with existing tropical satellite observations products (e.g., Spracklen et al., 2012).

4.2 EOFs reveal importance of land surfaces

Many studies suggest that land surface evaporation plays an important role for atmospheric flows of moisture (e.g., Tuinenburg et al., 2012; van der Ent et al., 2014). Our EOF analysis reveals that much of the variability (i.e., EOF1) in evaporation contribution can be explained by changes in terrestrial source regions (rather than oceanic regions). To an

extent, this result is expected given that we explicitly selected sink regions that are dependent on terrestrial sources of evaporation. Nonetheless, our analysis further confirms the importance of terrestrial regions for driving the variability of rainfall in these sink regions.

The EOF analysis also provides additional information for the ongoing discussion of the sources of Sahelian precipitation (e.g., Druyan and Koster, 1989). Other work has suggested that the primary driver of changes in Sahelian precipitation is the adjacent Atlantic Ocean and that the closest land surfaces play a secondary role (e.g., Biasutti et al., 2008). Our findings could be complementary to this previous work in that they illustrate variability in the sources of evaporation (i.e., the *proximate* causes of the variation), whereas other work may identify the underlying dynamical drivers of variability (i.e., the *ultimate* causes of the variation). This may also connect with the ongoing discussion of the varying role of oceanic and terrestrial sources of moisture. Given that other research has found terrestrial regions to be comparatively important during dry versus wet years (e.g., Brubaker et al., 2001; Chan and Misra, 2010; Bosilovich and Chern, 2006; Spracklen et al., 2012), a detailed seasonal and regional analysis of proximate versus ultimate causation in precipitationshed variability may be instructive, though it is outside the scope of this present analysis.

4.3 Governance of the core precipitationshed

In this work we identified the core precipitationshed as the evaporation source region that contributes a significant amount of evaporation to sink region precipitation, every year. Given the persistence of the core precipitationshed for multiple sink regions, we suggest that it is reasonable to discuss the practical next steps for advancing the discussion of precipitationshed governance.

Recent studies have quantified how anthropogenic land cover change influences the hydrological cycle through land cover change impacts on evaporation rates (e.g., Gordon et al., 2005; Sterling et al., 2012), and the eventual precipitation that falls downwind (e.g., Lo and Famiglietti, 2013). However, land cover change has the potential to influence not only evaporation rates but also the atmospheric circulation itself. In some cases, this effect has been shown to be small (e.g., Bagley et al., 2014), while in others land cover change leads to significantly different circulation patterns (e.g., Goessling and Reick, 2011; Lo and Famiglietti, 2013; Tuinenburg et al., 2014). If one is to apply the precipitationshed framework to understanding how land cover change may influence downwind precipitation, then it will be important to address whether the circulation itself is significantly modified. If this is the case, new precipitationshed boundaries will need to be identified to reflect the modified circulation.

A logical next step could be to identify current land uses and discuss past, current, and future land-use policies that

can influence moisture recycling in the precipitationshed. Understanding key actors within the precipitationshed would also be important. Keys et al. (2012) contributed to this effort by exploring the vulnerability of sink regions to land-use changes in the precipitationshed, by considering both historic and potential future land-use changes, as well as population and number of countries within a precipitationshed. The authors assigned a qualitative score to each sink region, based on the vulnerability assessment, but stopped short of exploring the implications for future governance. This work moves this discussion forward both by quantifying the variability of the precipitationshed and by defining a core precipitationshed, which could be used as the spatial unit of moisture recycling governance.

5 Conclusions

Keys et al. (2012) introduced the concept of the precipitationshed as a potential tool for assessing upwind land-use change impacts on a given region's precipitation. In this work we quantify the spatial interannual variability of three precipitationsheds and examine whether spatial and temporal variability are robust across two separate reanalysis data sets. Specifically, we find that

- the reanalysis data sets agree reasonably well, for two of the three regions;

- a core precipitationshed exists, whereby a large fraction of the precipitationshed contributes a substantial amount of evaporation to the sink region every year;

- most of the interannual variability in the precipitationshed is explained by a pulsing of more (or less) evaporation from the core terrestrial precipitationshed.

Our finding that a core, persistent precipitationshed exists implies that the precipitationshed boundary may be useful for describing terrestrial sources of a region's precipitation. Likewise, our statistical analysis revealed that much of the variability in growing-season precipitation arises from a pulsing of evaporation from the core terrestrial precipitationshed. This suggests that the land surface plays a dominant role in mediating variability in moisture recycling processes in these regions. Thus, there is likely a biophysical basis for the coordination and governance of land-use change within the precipitationshed.

Finally, understanding what causes precipitation to increase or decrease is of paramount importance to rainfed agriculture, which is tasked with feeding 3 billion more people by 2050 (e.g., Rockström et al., 2010). Our analysis provides critical information towards this understanding, by clearly identifying the importance of persistent, terrestrial sources of evaporation for regions dependent on rainfed agriculture.

The Supplement related to this article is available online at doi:10.5194/hess-18-3937-2014-supplement.

References

Bagley, J. E., Desai, A. R., Dirmeyer, P. A., and Foley, J. A.: Effects of land cover change on moisture availability and potential crop yield in the world's breadbaskets, Environ. Res. Lett., 7, 014009, doi:10.1088/1748-9326/7/1/014009, 2012.

Bagley, J. E., Desai, A. R., Harding, K. J., Snyder, P. K., and Foley, J. A.: Drought and Deforestation: Has land cover change influenced recent precipitation extremes in the Amazon?, J. Climate, 27, 345–361, doi:10.1175/JCLI-D-12-00369.1, 2014.

Biasutti, M., Held, I. M., Sobel, A. H., and Giannini, A.: SST Forcings and Sahel Rainfall Variability in Simulations of the Twentieth and Twenty-First Centuries, J. Climate, 21, 3471–3486, doi:10.1175/2007JCLI1896.1, 2008.

Bosilovich, M. and Chern, J. D.: Simulation of water resources and precipitation recycling for the MacKenzie, Mississippi, and Amazon River basins, J. Hydromet., 7, 312–329, 2006.

Bosilovich, M. G., Robertson, F. R., and Chen, J.: Global Energy and Water Budgets in MERRA, J. Climate, 24, 5721–5739, doi:10.1175/2011JCLI4175.1, 2011.

Brubaker, K., Dirmeyer, P., Sudrajat, A., Levy, B. S., and Bernal, F.: A 36-yr climatological description of the evaporative sources of warm-season precipitation in the Mississippi River basin, J. Hydromet., 2, 537–557, doi::10.1175/1525-7541(2001)002<0537:AYCDOT>2.0.CO;2, 2001.

Chan, S. C. and Misra, V.: A Diagnosis of the 1979–2005 Extreme Rainfall Events in the Southeastern United States with Isentropic Moisture Tracing, Mon. Weather Rev., 138, 1172–1185, doi:10.1175/2009MWR3083.1, 2010.

Dee, D. P., Uppala, S. M., Simmons, A. J., Berrisford, P., Poli, P., Kobayashi, S., Andrae, U., Balmaseda, M. A., Balsamo, G., Bauer, P., Bechtold, P., Beljaars, A. C. M., van de Berg, L., Bidlot, J., Bormann, N., Delsol, C., Dragani, R., Fuentes, M., Geer, A. J., Haimberger, L., Healy, S. B., Hersbach, H., Hólm, E. V., Isaksen, L., Kå llberg, P., Köhler, M., Matricardi, M., McNally, A. P., Monge-Sanz, B. M., Morcrette, J. J., Park, B. K., Peubey, C., de Rosnay, P., Tavolato, C., Thépaut, J. N., and Vitart, F.: The ERA-Interim reanalysis: configuration and performance of the data assimilation system, Quart. J. Roy. Meteorol. Soc., 137, 553–597, doi:10.1002/qj.828, 2011.

Ding, Y. and Chan, J. C. L.: The East Asian summer monsoon: an overview, Meteorol. Atmos. Phys., 89, 117–142, doi:10.1007/s00703-005-0125-z, 2005.

Dirmeyer, P. A., Schlosser, C. A., and Brubaker, K. L.: Precipitation, Recycling, and Land Memory: An Integrated Analysis, J. Hydromet., 10, 278–288, doi:10.1175/2008JHM1016.1, 2009.

Dirmeyer, P. A., Jin, Y., Singh, B., and Yan, X.: Trends in Land – Atmosphere Interactions from CMIP5 Simulations, J. Hydromet., 14, 829–849, doi:10.1175/JHM-D-12-0107.1, 2013a.

Dirmeyer, P. A., Wei, J., Bosilovich, M. G., and Mocko, D. M.: Comparing Evaporative Sources of Terrestrial Precipitation and Their Extremes in MERRA Using Relative Entropy, J. Hydromet., 15, 102–116, doi:10.1175/JHM-D-13-053.1, 2013b.

Dominguez, F., Villegas, J. C., and Breshears, D. D.: Spatial extent of the North American Monsoon: Increased cross-regional linkages via atmospheric pathways, Geophys. Res. Lett., 36, L07401, doi:10.1029/2008gl037012, 2009.

Drumond, A., Nieto, R., Gimeno, L., and Ambrizzi, T.: A Lagrangian identification of major sources of moisture over Central Brazil and La Plata Basin, J. Geophys. Res., 113, D14128, doi:10.1029/2007jd009547, 2008.

Druyan, L. M. and Koster, R. D.: Sources of Sahel Precipitation for Simulated Drought and Rainy Seasons, J. Climate, 2, 1438–1446, 1989.

Eltahir, E. and Bras, R.: Precipitation recycling in the Amazon basin, Quart. J. Roy. Meteorol. Soc., 120, 861–880, 1994.

Ferreira-Pires, G. F. and Costa, M. H.: Deforestation causes different subregional effects on the Amazon bioclimatic equilibrium, Geophys. Res. Lett., 40, 3618–3623, doi:10.1002/grl.50570, 2013.

Giannini, A., Salack, S., Lodoun, T., Ali, A., Gaye, A. T., and Ndiaye, O.: A unifying view of climate change in the Sahel linking intra-seasonal, interannual and longer time scales, Environ. Res. Lett., 8, 1–8, doi:10.1088/1748-9326/8/2/024010, 2013.

Gimeno, L., Stohl, A., Trigo, R. M., Dominguez, F., Yoshimura, K., Yu, L., Drumond, A., Durán-Quesada, A. M., and Nieto, R.: Oceanic and Terrestrial Sources of Continental Precipitation, Rev. Geophysics, 50, RG4003, doi:10.1029/2012RG000389, 2012.

Goessling, H. F. and Reick, C. H.: What do moisture recycling estimates tell us? Exploring the extreme case of non-evaporating continents, Hydrol. Earth Syst. Sci., 15, 3217–3235, doi:10.5194/hess-15-3217-2011, 2011.

Goessling, H. F. and Reick, C. H.: On the "well-mixed" assumption and numerical 2-D tracing of atmospheric moisture, Atmos. Chem. Phys., 13, 5567–5585, doi:10.5194/acp-13-5567-2013, 2013.

Gordon, L. J., Steffen, W., Jönsson, B. F., Folke, C., Falkenmark, M., and Johannessen, A.: Human modification of global water vapor flows from the land surface, Proc. Nat. Acad. Sci. USA, 102, 7612–7617, doi:10.1073/pnas.0500208102, 2005.

Hartmann, D. and Lo, F.: Wave-driven zonal flow vacillation in the Southern Hemisphere, J. Atmos. Sci., 55, 1303–1315, 1998.

Keys, P. W., van der Ent, R. J., Gordon, L. J., Hoff, H., Nikoli, R., and Savenije, H. H. G.: Analyzing precipitationsheds to understand the vulnerability of rainfall dependent regions, Biogeosciences, 9, 733–746, doi:10.5194/bg-9-733-2012, 2012.

Koster, R., Jouzel, J., Suozzo, R., Russell, G., Broecker, W., Rind, D., and Eagleson, P.: Global sources of local precipitation as determined by the NASA/GISS GCM, Geophys. Res. Lett., 13, 121–124, 1986.

Lettau, H., Lettau, K., and Molion, L. C.: Amozonia's hydrological cycle and the role of atmospheric recycling in assessing deforestation effects, Mon. Weather Rev., 107, 227–238, 1979.

Lo, M. and Famiglietti, J. S.: Irrigation in California's Central Valley strengthens the southwestern U.S. water cycle, Geophys. Res. Lett., 40, 301–306, doi:10.1002/grl.50108, 2013.

Lorenz, C. and Kunstmann, H.: The Hydrological Cycle in Three State-of-the-Art Reanalyses: Intercomparison and Performance Analysis, J. Hydromet., 13, 1397–1420, doi:10.1175/JHM-D-11-088.1, 2012.

North, G., Bell, T., Cahalan, R., and Moeng, F.: Sampling errors in the estimation of empirical orthogonal functions, Mon. Weather Rev., 110, 699–706, 1982.

Numaguti, A.: Origin and recycling processes of precipitating water over the Eurasian continent: experiments using an atmospheric general circulation model, J. Geophys. Res., 104, 1957–1972, 1999.

Portmann, F., Siebert, S., and Döll, P.: Global monthly irrigated and rainfed crop areas around the year 2000: a new high-resolution data set for agricultural and hydrological modeling, Global Biogeochem. Cy., 24, GB1011, doi:10.1029/2008GB003435, 2010.

Reale, O., Feudale, L., and Turato, B.: Evaporative moisture sources during a sequence of floods in the Mediterranean region, Geophys. Res. Lett., 28, 2085–2088, doi:10.1029/2000GL012379, 2001.

Rienecker, M. M., Suarez, M. J., Gelaro, R., Todling, R., Bacmeister, J., Liu, E., Bosilovich, M. G., Schubert, S. D., Takacs, L., Kim, G.-K., Bloom, S., Chen, J., Collins, D., Conaty, A., da Silva, A., Gu, W., Joiner, J., Koster, R. D., Lucchesi, R., Molod, A., Owens, T., Pawson, S., Pegion, P., Redder, C. R., Reichle, R., Robertson, F. R., Ruddick, A. G., Sienkiewicz, M., and Woollen, J.: MERRA: NASA's Modern-Era Retrospective Analysis for Research and Applications, J. Climate, 24, 3624–3648, doi:10.1175/JCLI-D-11-00015.1, 2011.

Rios-Entenza, A. and Miguez-Macho, G.: Moisture recycling and the maximum of precipitation in spring in the Iberian Peninsula, Clim. Dynam., 42, 3207–3231, doi:10.1007/s00382-013-1971-x, 2013.

Risi, C., Noone, D., Frankenberg, C., and Worden, J.: Role of continental recycling in intraseasonal variations of continental moisture as deduced from model simulations and water vapor isotopic measurements, Water Resour. Res., 49, 4136–4156, doi:10.1002/wrcr.20312, 2013.

Rockström, J., Karlberg, L., Wani, S. P., Barron, J., Hatibu, N., Oweis, T., Bruggeman, A., Farahani, J., and Qiang, Z.: Managing water in rainfed agriculture: The need for a paradigm shift, Agr. Water Manage., 97, 543–550, doi:10.1016/j.agwat.2009.09.009, 2010.

Rowell, D.: The impact of Mediterranean SSTs on the Sahelian rainfall season, J. Climate, 16, 849–862, 2003.

Salih, A. A. M., Körnich, H., and Tjernström, M.: Climate impact of deforestation over South Sudan in a regional climate model, Int. J. Climatol., 33, 2362–2375, doi:10.1002/joc.3586, 2013.

Savenije, H. H. G.: New definitions for moisture recycling and the relationship with land-use changes in the Sahel, J. Hydrol., 167, 57–78, 1995.

Sodemann, H., Schwierz, C., and Wernli, H.: Interannual variability of Greenland winter precipitation sources: Lagrangian moisture diagnostic and North Atlantic Oscillation influence, J. Geophys. Res. Atmos., 113, D03107, doi:10.1029/2007jd008503, 2008.

Spracklen, D. V., Arnold, S. R., and Taylor, C. M.: Observations of increased tropical rainfall preceded by air passage over forests, Nature, 489, doi:10.1038/nature11390, 2012.

Sterling, S. M., Ducharne, A., and Polcher, J.: The impact of global land-cover change on the terrestrial water cycle, Nature Climate Change, 3, 385–390, doi:10.1038/nclimate1690, 2012.

Thompson, D. and Wallace, J.: The Arctic Oscillation signature in the wintertime geopotential height and temperature fields, Geophys. Res. Lett., 25, 1297–1300, 1998.

Trenberth, K. E., Fasullo, J. T., and Mackaro, J.: Atmospheric Moisture Transports from Ocean to Land and Global Energy Flows in Reanalyses, J. Climate, 24, 4907–4924, doi:10.1175/2011JCLI4171.1, 2011.

Tuinenburg, O. A., Hutjes, R. W. A., and Kabat, P.: The fate of evaporated water from the Ganges basin, J. Geophys. Res., 117, D01107, doi:10.1029/2011JD016221, 2012.

Tuinenburg, O. A., Hutjes, R. W. A., Stacke, T., Wiltshire, A., and Lucas-Picher, P.: Effects of Irrigation in India on the Atmospheric Water Budget, J. Hydromet., 15, 1028–1050, doi:10.1175/JHM-D-13-078.1, 2014.

van der Ent, R. J. and Savenije, H. H. G.: Oceanic sources of continental precipitation and the correlation with sea surface temperature, Water Resour. Res., 49, 3993–4004, doi:10.1002/wrcr.20296, 2013.

van der Ent, R. J., Savenije, H. H., Schaefli, B., and Steele-Dunne, S. C.: Origin and fate of atmospheric moisture over continents, Water Resour. Res., 46, W09525, doi:10.1029/2010WR009127, 2010.

van der Ent, R. J., Coenders-Gerrits, A. M. J., Nikoli, R., and Savenije, H. H. G.: The importance of proper hydrology in the forest cover-water yield debate: commentary on Ellison et al. (2012) (Global Change Biology, 18, 806–820), Glob. Change Biol., 18, 2677–2680, 2012.

van der Ent, R. J., Tuinenburg, O. A., Knoche, H.-R., Kunstmann, H., and Savenije, H. H. G.: Should we use a simple or complex model for moisture recycling and atmospheric moisture tracking?, Hydrol. Earth Syst. Sci., 17, 4869–4884, doi:10.5194/hess-17-4869-2013, 2013.

van der Ent, R. J., Wang-Erlandsson, L., Keys, P. W., and Savenije, H. H. G.: Contrasting roles of interception and transpiration in the hydrological cycle – Part 2: Moisture recycling, Earth Syst. Dynam. Discuss., 5, 281–326, doi:10.5194/esdd-5-281-2014, 2014.

Wei, J., Dirmeyer, P. A., Wisser, D., Bosilovich, M. G., and Mocko, D. M.: Where Does the Irrigation Water Go? An Estimate of the Contribution of Irrigation to Precipitation Using MERRA, J. Hydromet., 14, 275–289, doi:10.1175/JHM-D-12-079.1, 2013.

Yoshimura, K., Oki, T., Ohte, N., and Kanae, S.: Colored moisture analysis estimates of variations in 1998 Asian monsoon water sources, J. Meteor. Res. Japan, 82, 1315–1329, 2004.